

Supplemental Figures

Figure S1

A

PROM-1	1	MDKSTPRRTYNLRSDRTTQNSPVSRSQLENHRNASVSLRKRNSATEERCSSRKRRTTQOT
Cbr-PROM-1	1	MNQATP-RRYNLRSSQRDVPI---P---YNSAKSVVPLRKRNSPSEANKGHRQRTQOS
F54D5.9	1	MFRTE-PPFRLLARKRNSDSTPPITKFF---ATVKRERSSESSESKN-----VCQK
Human-FBXO47	1	MASRTN-TNETLIP-----NQKLRRSNRQTSC-----YSKT
Mouse-FBXO47	1	MASRVN-TSETLIP-----KQKCRSNHHSY-----FCNT
PROM-1	61	HGLPFSSPDAINHQ-----RAFHLDEHKVCSKLTTRLISI---EVETSYGSEFGKLPY
Cbr-PROM-1	53	HGPPERSPAGIDLPE-----RQSHIEQRP-IVQLPTRLSR---ELEQPFCSFGQLPN
F54D5.9	48	LDESEFAPNNLSQTSHTDSPDNGLLYSLEDLRALLGVVFKFSKCVSPSPAPVGLLENLPN
Human-FBXO47	31	LGSGEQFIS-----TFGNFKALPL
Mouse-FBXO47	31	LDSDPQLLS-----TLCNFKVLPL
PROM-1	109	DAVIHLLTRTPYNLLSRMVMSTSCWNQTIGAYMRSAGFRERWLLDIDIA---ES-----
Cbr-PROM-1	100	DVIYOILSRTPYTLLGRMSMTSTVWKRTISAYVRSGSENLRLTKDVENT---MDSFSNEK
F54D5.9	108	RAYSHLETITDMQSINALSTSTKLCSRVKTYVSTHDFRRMQLDNLDFNSSLRPDDEE
Human-FBXO47	50	EIFQIITKYL SVKDISMLSMVSKTVSOHIINYYISTSSGSKRLLLQDFHNLDELDRRQDSA
Mouse-FBXO47	50	EILHIITRYL SVKDIGMLSMVSKTVSOHIINYYISTSSGSKRLLLQNFHDIDLEGTKEETA
PROM-1	160	SKPLDPFFDMGKILVRCLTINYEWKARIDCLKSFMTL-----AYESGALIAAGLG
Cbr-PROM-1	157	LGSNDLYFSMGTLTKYLTINEKWSVRLDCLRMFLTM-----AYEADSSIAGIG
F54D5.9	168	FLENDPFTACGGLIKSIITITMNTKIRAQVFLN-----ICRNLRDQLGGS LHGFG
Human-FBXO47	110	IL--EHVRSILGLLFKRCITLLPTKERIKYIHKILTEVSCFKFNGCAAPMQC--LGLTCYG
Mouse-FBXO47	110	LL--EHVRAIGLLLFKRCITLLPTKERIKYIHKILSEVSCFKFSGCSVPQLQC--LGLSCYG
PROM-1	208	KMIHAFENRPFDEDIVLEQIDDIIVAMLLALVSGLKDDISAVLFTPETDRELEELDNMPILR
Cbr-PROM-1	205	KIVHAFALRPDEEIVMEEIDDIIVTLVFSIVGSLVHELNGVVSRSDVERDLENTENAHWF
F54D5.9	217	RLLETITHNWKFSE---RRIMVKAAMIDADLRPSITKVLTL-----AKPGQLIG
Human-FBXO47	166	MFLQTLTAGWDELE---CHRVYNFL-CELTNLCRKIQMAVC-----SKPGSAQK
Mouse-FBXO47	166	MFLQTLTAGWDELE---CHRVYNFL-CELTNLSRKMOTVVC-----NKPGSARK
PROM-1	268	EEMKLRKKTLNLFNNGSS---DEAHG-VNKYFLSLMKVFKTAHNAALPTAFYLLFSP
Cbr-PROM-1	265	YEMELRKRVLTLFLNNGVT---DPAVG-LNKFFLSVLRKFEKAHGVPVPTSLIYLLFSP
F54D5.9	263	LEMKVRSGLTOLFLNLSQDIDEASEQEIIEFGSWLSVLIRNV---IEKYQKGFYIYLFGP
Human-FBXO47	211	LELRIRLFCRNVLLDHWT-----HRSDSAFAWLTRILKPW---PMVNQARLLYIIFGP
Mouse-FBXO47	211	LELRVRLFCRNVLLDHWT-----HRSDSAFAWLTRILKPW---PMVNQARLLYIIFGP
PROM-1	323	TTIQDDEEVIHWHRLSLLSVVTSEEAEELKPLSRAMCATIQ-----CRNLKHV
Cbr-PROM-1	320	TTIYEGEEVIHWHRLSLOISVVDFDDALELNPLARAFALLO-----CKKLNN
F54D5.9	320	TRSSRIGERVWDWAYFCEDDSDT---FTLRKSEPNYRKLLSTLLNGIRALRIMNNSKSSD
Human-FBXO47	260	ISPQ--DGQVWVQEMIEEPTDE---FSLKGLADAIKLLYDA-----ST
Mouse-FBXO47	260	TSPH--DGQVIWQEMIEGPTDE---SSLKGLANAIAKLLYDT-----GA
PROM-1	371	LPWSKNTIFNLME---EITTYENPWSMSTFVALNVLEPELVPI-----GVVARM--NRN
Cbr-PROM-1	368	LPWTKNTIFNLME---EITTYENPWSMNTFVALHVLPELVPI-----GVVARL--NRN
F54D5.9	376	QMWSGKKLYQLFLRIIEVCEVQGFWESETSSSMALADSSGLLSEYLVLT-CLDPRDDYET
Human-FBXO47	298	KEWTADDVISLVD---ELSVVEREWLLENNARLLMSGNNICFSFMASKAVNGRTIELAR
Mouse-FBXO47	298	KGWTADDVISLVD---ELSVVEREWLLENNARLLMSGNNICFTFMASKAVNGRAVELAR
PROM-1	420	HEDEAGDIICTMKMLLHRWMDVYGVMEIIDTIKAVLKPYORRILFDRCDW-----
Cbr-PROM-1	417	HEDEAGDMICTMKMLLFRWKMDVVGVIERALESIKTALKPEQCRTLEFDRCDW-----
F54D5.9	435	LQNEAAEMVCLVRNHLRYWSAAPATFLAEPLHHAF--NHLAQLDGHYDGCYKAFLEKIWN
Human-FBXO47	355	LV-VFLALVCEKELYCMDWTVRMMQKVCK---VF--STEVE-----RKNELQNVAN
Mouse-FBXO47	355	LV-VFLALVCEKELYCMDWTVRMMQKVCK---VF--STAAE-----RKSFLQSIAN
PROM-1	472	WHQRNIDEHNRQM---GH-FSDIRAEIESQIEVMPVMKLL-----
Cbr-PROM-1	469	WHQRNIDDLHRRLL---GQSAEEIRAEIESQIEVMPVMKLL-----
F54D5.9	493	VQSSRLKEMVKNATNTTECSEKIREELDGQLSMARLLTDISNTVVLHQIGFQLPNDLAAE
Human-FBXO47	400	AFACVTMEMLQSIMSG---DRDEDRSFLNLFHLVHAQA---NFHK-----EVLYL
Mouse-FBXO47	400	AFACVTMEMLQPVMSG---DRDDDRGFLNLFHLVHAQA---NFHK-----EVLYL
PROM-1		-----
Cbr-PROM-1		-----
F54D5.9	553	LVNDPLEEEEQLE
Human-FBXO47	445	TMTPLST----
Mouse-FBXO47	445	TMTAISS-----

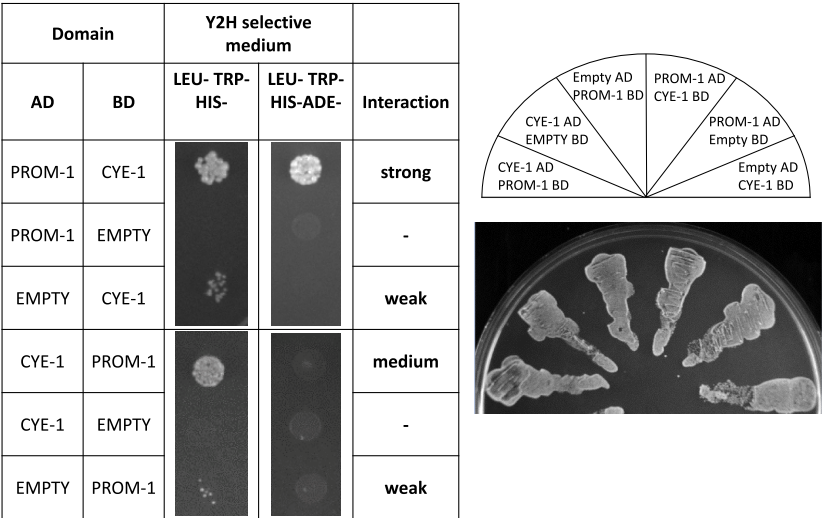


PROM-1 and its orthologs and homologs are F-box containing protein.

(A) Alignment of PROM-1 homologs. Proteins were aligned using Clustal Omega (www.ebi.ac.uk/Tools/msa/clustalo/). Colored lines represent the F-box motif (see panel B) in PROM-1 homologs (red - PROM-1, green - Cbr-PROM-1, purple - F54D5.9, blue - Human-FBXO47 and black - Mouse-FBXO47) (Jantsch *et al.* 2007). *C. elegans* PROM-1 and its paralog F54D5.9, as well as *C. briggsae* PROM-1 (Cbr-PROM-1), show conservation across almost the full-length of mammalian FBXO47; PROM-1 has slightly less than 20% sequence identity to human FBXO47 while F54D5.9 has slightly more than 20% sequence identity.

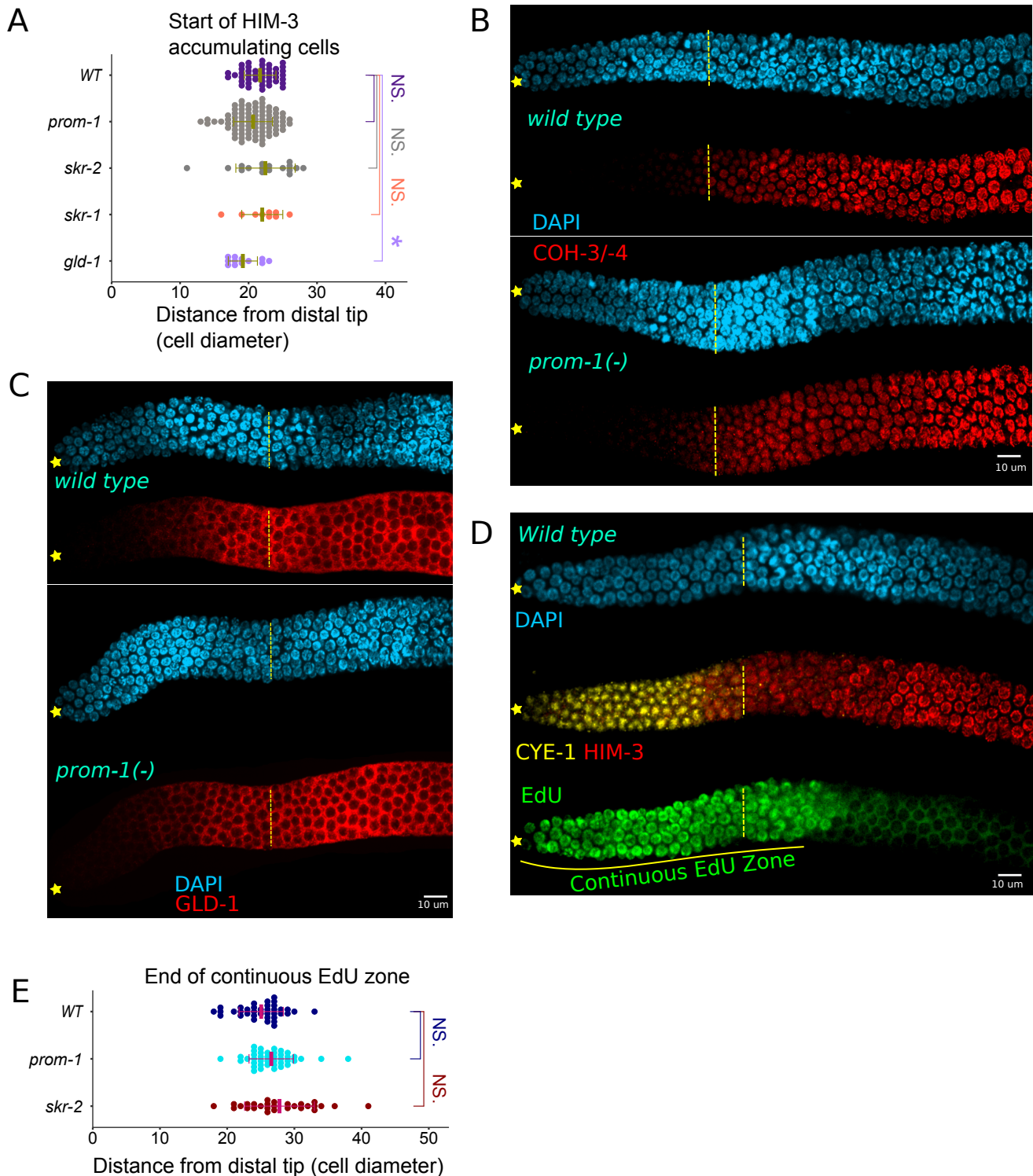
(B) Alignment of F-box motif of PROM-1 and other F-box proteins. The F-box motif lacks a strict consensus, with the most conserved residues found in ~80 - 95% of F-box containing proteins (Kipreos and Pagano 2000). The PROM-1 F-box motif is aligned (Clustal Omega) with predicted F-box motifs from PROM-1 orthologs, *C. elegans* and mammalian F-box proteins identified using <https://prosite.expasy.org/scanprosite/>. We note that this program fails to retrieve the F-box motif in *C. elegans* PROM-1, but does retrieve it from Cbr-PROM-1 and Cre-PROM-1 orthologs. Importantly, PROM-1 contains conserved residues at the least variable positions (below the alignment, in green) - leucine (position 8), proline (position 9), isoleucine (position 16) and serine (position 32), where positions are defined in Kipreos and Pagano (2000) [note the F-box from ScanProsite is 1 residue shorter at the N-terminus than F-box defined in Kipreos and Pagano 2000]. While PROM-1 does not have leucine or methionine at residue 20, these residues are not observed in 19% of F-box motif containing proteins (Kipreos and Pagano 2000), and thus shows variability, as also observed in LIN-23 and FOG-2.

Figure S2



Yeast two-hybrid analysis showing the interaction between PROM-1 and CYE-1.
Yeast strains contain GAL4 activation domain (AD) and DNA-binding domain (BD) vectors with no insert (empty), full-length *cye-1* cDNA or full-length *prom-1* cDNA. Strain growth was tested on both medium stringency (Leu- Trp- His-) and high stringency (Leu- Trp- His- Ade-) plates. Growth on Leu- Trp- medium (right panel) indicates successful transformation of both the AD and BD plasmids. The interaction between CYE-1 and PROM-1 was tested with CYE-1 in the BD plasmid and PROM-1 in the AD plasmid, and *vice versa*. Importantly, interaction was observed in both directions. However, as sometimes is observed in the yeast two-hybrid assay, the interaction is stronger in one direction than the other; the interaction was stronger with PROM-1 in the AD plasmid, and CYE-1 in the BD plasmid, as growth was observed on both the medium and high stringency plates. (left panel).

Figure S3



Spatial position of accumulation of a subset of meiotic entry markers in SCF^{PROM-1} mutant germlines is similar to wild type.

(A) Graph showing distance, in cell diameters, between the distal end of the germline and overt meiotic entry, which we define here as the first row of cells where >50% of nuclei are HIM-3 positive, in young adult hermaphrodites for the indicated genotype. The position of meiotic entry in *prom-1*, *skr-1* and *skr-2* single mutants is similar to wild type. The position of meiotic entry in *gld-1* mutant germlines is shifted towards the distal end due to its smaller progenitor zone, compared to WT (Brenner and Schedl 2016).

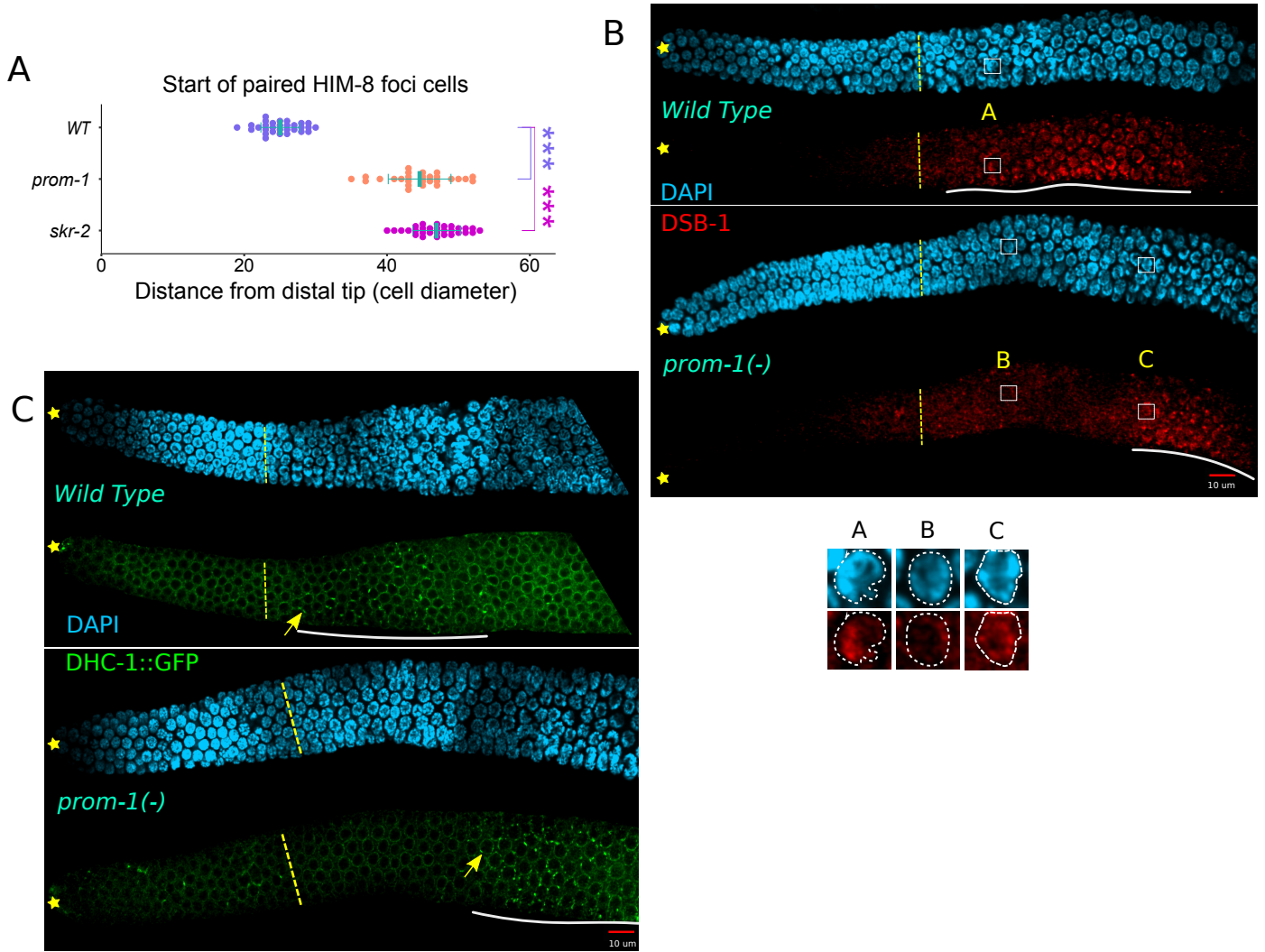
(B, C) Images of (B) COH-3/-4-stained (red) and (C) GLD-1-stained (red), distal germlines of dissected young adult hermaphrodites, co-stained with DAPI (cyan) for the indicated genotype. Asterisks, distal gonadal end. Dashed yellow lines, position of overt meiotic entry.

(D) Images of distal germline of a dissected wild type young adult hermaphrodite, top panel, DAPI (cyan); middle panel, CYE-1 (yellow) and HIM-3 (red); bottom panel, EdU (green). Asterisks, distal gonadal end. Dashed yellow lines, position of overt meiotic entry. Solid yellow line, continuous EdU zone. The continuous EdU zone, for this study, is defined as the number of rows from the distal end of the germline to the most proximal row of germ cells where all nuclei display EdU staining after a 4-hour growth on EdU bacteria. The continuous EdU zone is generally about 4-5 cell diameter longer than the steady-state size of progenitor zone, since a 4-hour EdU pulse labels some meiotic S-phase cells that enter meiosis during the experimental time window (Fox *et al.* 2011).

(E) Graph showing the distribution of continuous EdU zone lengths from the distal tip for the indicated genotypes.

For (A) and (E), data are plotted as horizontal dotplots with each dot representing length in cell diameter for one germline. Thick vertical lines represent mean and horizontal lines represent mean \pm std deviation. Statistical significance was determined using either two-tailed Student's T-test (for $n < 30$) or Z-test (for $n \geq 30$). p-value ≤ 0.01 = significant (*), p-value ≤ 0.001 = very significant (**), p-values ≤ 0.0001 = extremely significant (***) and p-values > 0.01 = non-significant (NS.).

Figure S4



Chromosome pairing is defective at meiotic entry in SCF^{PROM-1} mutant germlines.

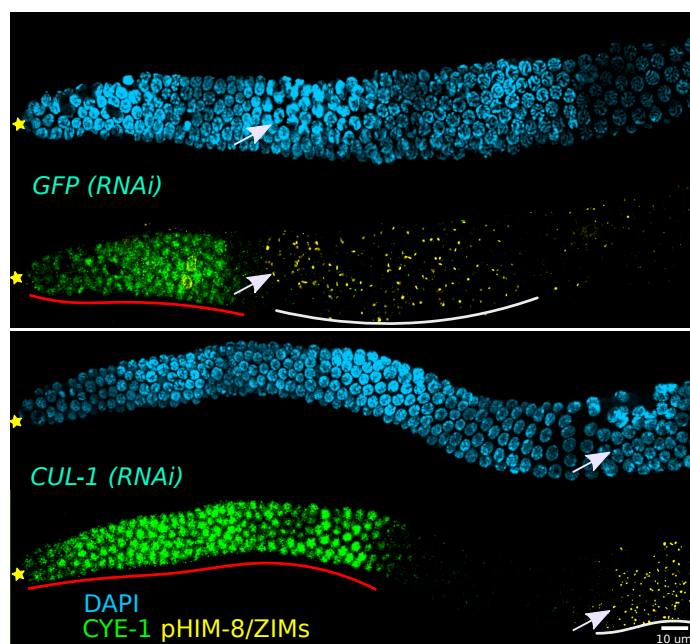
(A) Graph showing distance, in cell diameters, from distal tip of germline to the first cell row where HIM-8 strong foci (paired) appear, in young adult hermaphrodites of the indicated genotype. Data are plotted as horizontal dotplots with each dot representing length in cell diameter for one gonad. Thick vertical lines represent mean and horizontal lines represent mean \pm std deviation. Statistical significance was determined using either two-tailed Student's T-test (for $n < 30$) or Z-test (for $n \geq 30$). p-value ≤ 0.01 = significant (*), p-value ≤ 0.001 = very significant (**), p-values ≤ 0.0001 = extremely significant (***) and p-values > 0.01 = non-significant (NS).

(B) Images of DSB-1-stained (red) distal germlines from dissected young adult hermaphrodites, co-stained with DAPI (cyan). Asterisks, distal gonadal end. Dashed yellow lines, position of overt meiotic entry. Solid white lines, show start and positions of strong and chromatin-colocalized DSB-1 foci accumulation. Note the weaker DSB-1 staining between meiotic entry and start of white line, in both genotypes, which is not necessarily chromatin-enriched. Inset A: a nucleus in wild type germline with strong chromatin-enriched DSB-1 staining. Inset B: a nucleus in *prom-1* mutant germline with weak DSB-1 staining and is not chromatin-enriched. Inset C: a proximal nucleus in *prom-1* mutant germline with strong chromatin-enriched DSB-1 staining.

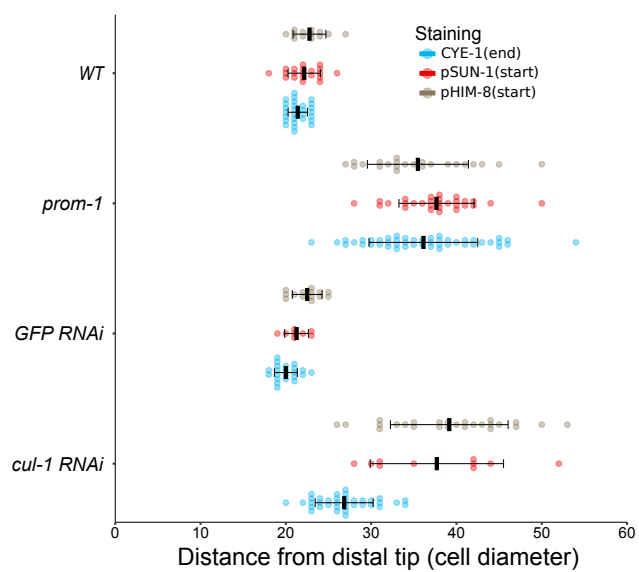
(C) Images of DHC-1::GFP (green) stained distal germlines from dissected young adult hermaphrodites, co-stained with DAPI (cyan) for the indicated genotype. Asterisks, distal end of gonad. Dashed yellow lines, position of overt meiotic entry. Solid white lines show start and positions of DHC-1::GFP nuclear envelop aggregate accumulation. Arrows, nuclei with DHC-1::GFP aggregates on the external surface of the nuclear envelope.

Figure S5

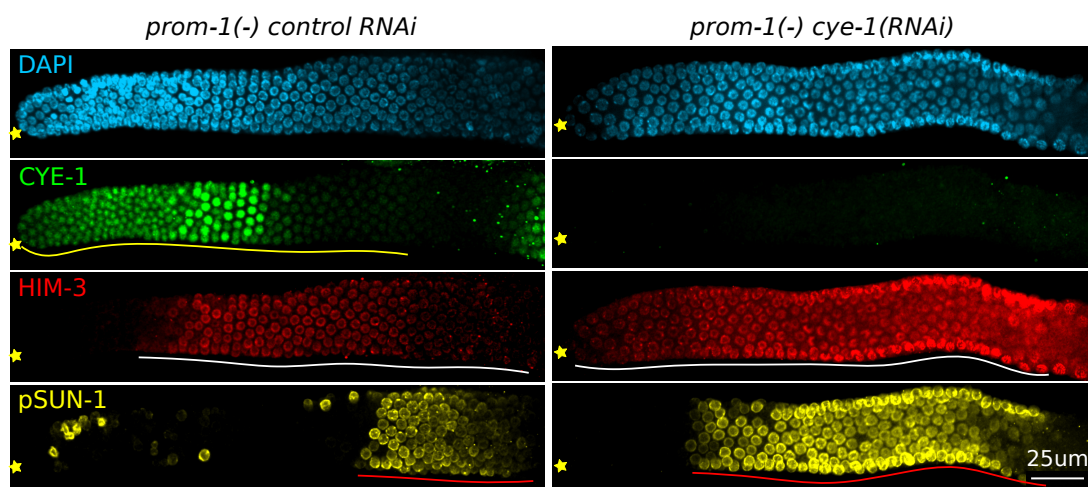
A



B



C



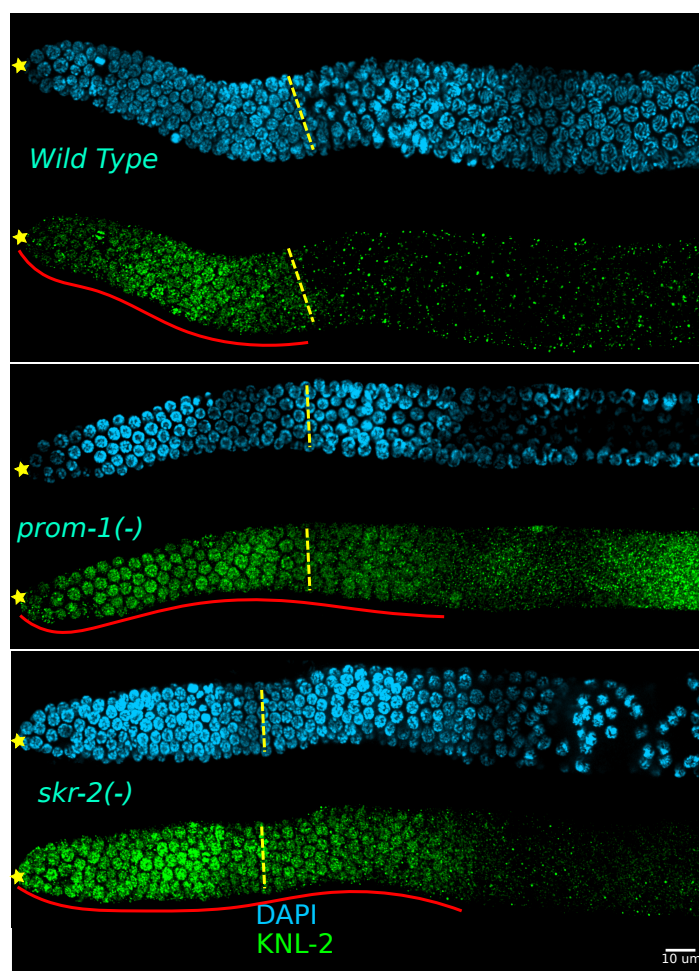
Absence of CHK-2 activity at meiotic entry is not due ectopic CYE-1 in SCF^{PROM-1} loss of function germlines.

(A) Images of dissected germlines of young adult hermaphrodites of the indicated genotypes stained with antibody against CYE-1 (green), pHIM-8/ZIMs (yellow) and DAPI (cyan). Asterisks, distal gonadal end. Dashed yellow lines, position of overt meiotic entry. White lines, start and proximal progression of pHIM-8/ZIMs positive nuclei. Solid red lines, CYE-1 accumulation. In the *cul-1* RNAi germline, note the gap between the proximal end of ectopic CYE-1 accumulation (right end of red line) and the distal end of the beginning of delayed distal pHIM-8/ZIM (left end of the white line). Arrows, nuclei with pHIM-8/ZIMs staining.

(B) Graph showing distance, in cell diameters, from distal tip of the germline to the most proximal row of cells (end) for CYE-1 staining, and the most distal row of cells (start) for pSUN-1 and pHIM-8/ZIMs positive germ cells, for young adult hermaphrodite of the indicated genotype. Data are plotted as horizontal dotplots with each dot representing length in cell diameter for one gonad. Thick vertical lines represent mean and horizontal lines represent mean \pm std deviation.

(C) Images of dissected germlines from young adult hermaphrodites of the indicated genotype, stained for HIM-3 (red), CYE-1 (green), pSUN-1 (yellow) and DAPI (cyan). Asterisks, distal gonadal end. Solid yellow lines, CYE-1 accumulation. Solid white lines, HIM-3 accumulation. Solid red lines, pSUN-1 accumulation. Mid-L4 *prom-1*(-) worms were subjected to either control RNAi (GFP, left panel) or against *cye-1* (right panel). After 66 hours of RNAi, the worms were dissected and stained. Although CYE-1 has completely disappeared following RNAi and all the cells in the distal end of the germline have entered meiosis (HIM-3+), pSUN-1 staining is still absent from the distal most ~ 10 diameter of the distal germline, indicating that pairing has not occurred in this region. In the control RNAi germline shown, following the region of high ectopic CYE-1, CYE-1 levels decrease, but remain significantly above background, as indicated with the yellow line.

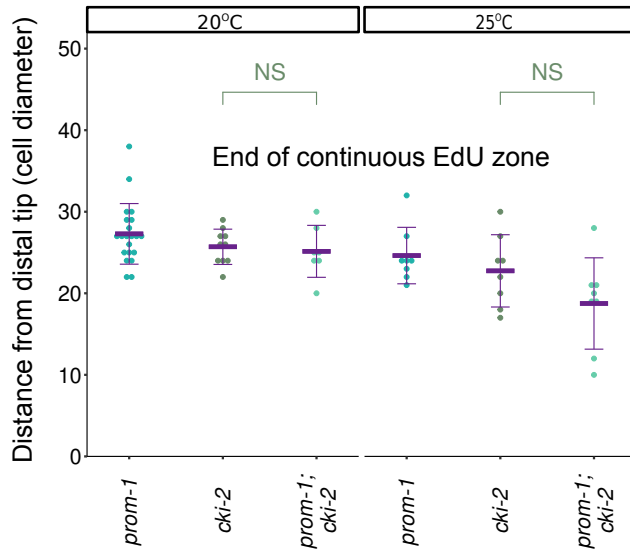
Figure S6



Ectopic accumulation of KNL-2 in SCF^{PROM-1} mutants.

Images of KNL-2-stained (green) distal germlines from dissected young adult hermaphrodites, co-stained with DAPI (cyan) for the indicated genotype. Asterisks, distal gonadal end. Dashed yellow lines, position of overt meiotic entry. Solid red lines, zone of continuous KNL-2 protein accumulation.

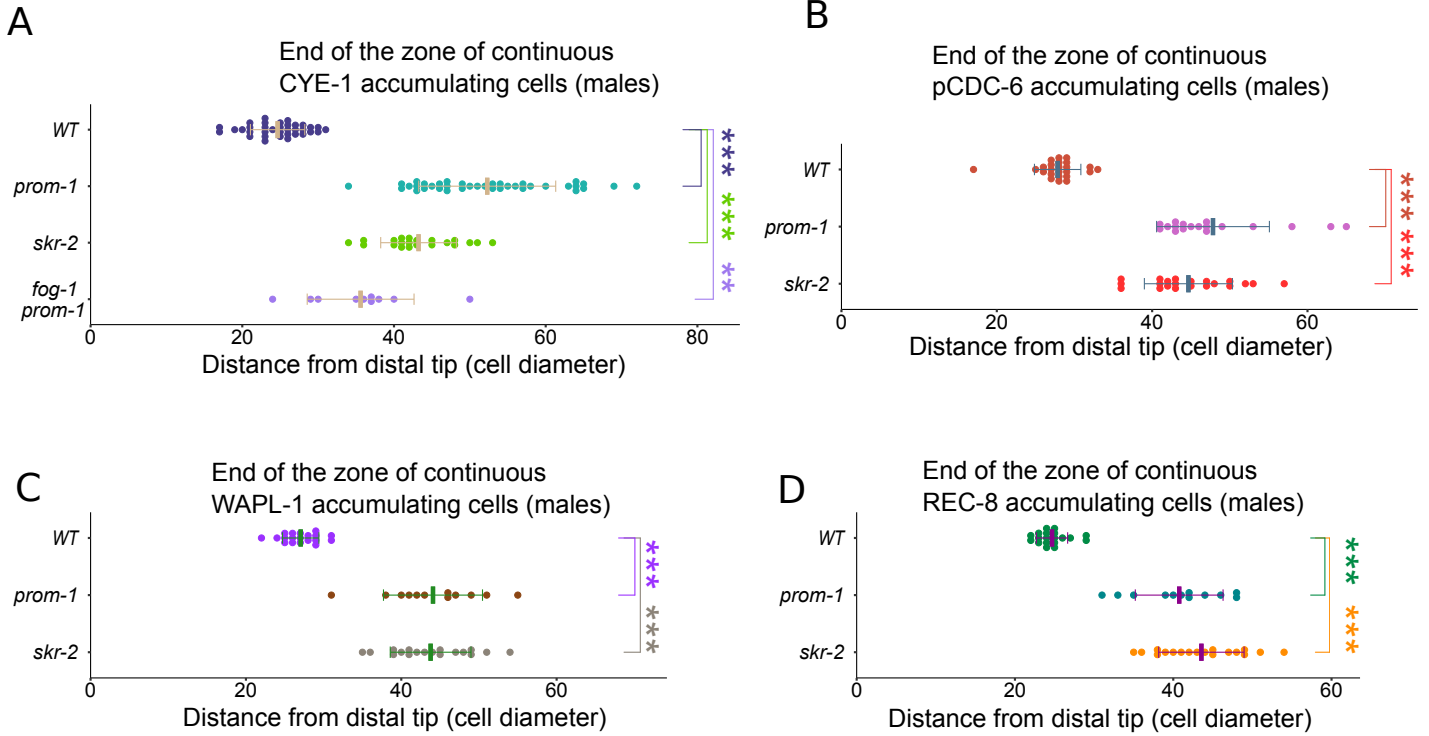
Figure S7



CDK inhibitor CKI-2 is not responsible for mitotic quiescence of germ cells that inappropriately accumulate CYE-1 in *prom-1* mutants.

Graph showing continuous EdU zone lengths for the indicated genotypes and temperatures, in cell diameters, from the distal tip. Data are plotted as dotplots with each dot representing length in cell diameter for one gonad. Thick horizontal lines represent mean and vertical lines represent mean \pm std deviation. Statistical significance was determined using either two-tailed Student's T-test (for $n < 30$) or Z-test (for $n \geq 30$). p-value ≤ 0.01 = significant (*), p-value ≤ 0.001 = very significant (**), p-values ≤ 0.0001 = extremely significant (***) and p-values > 0.01 = non-significant (NS.).

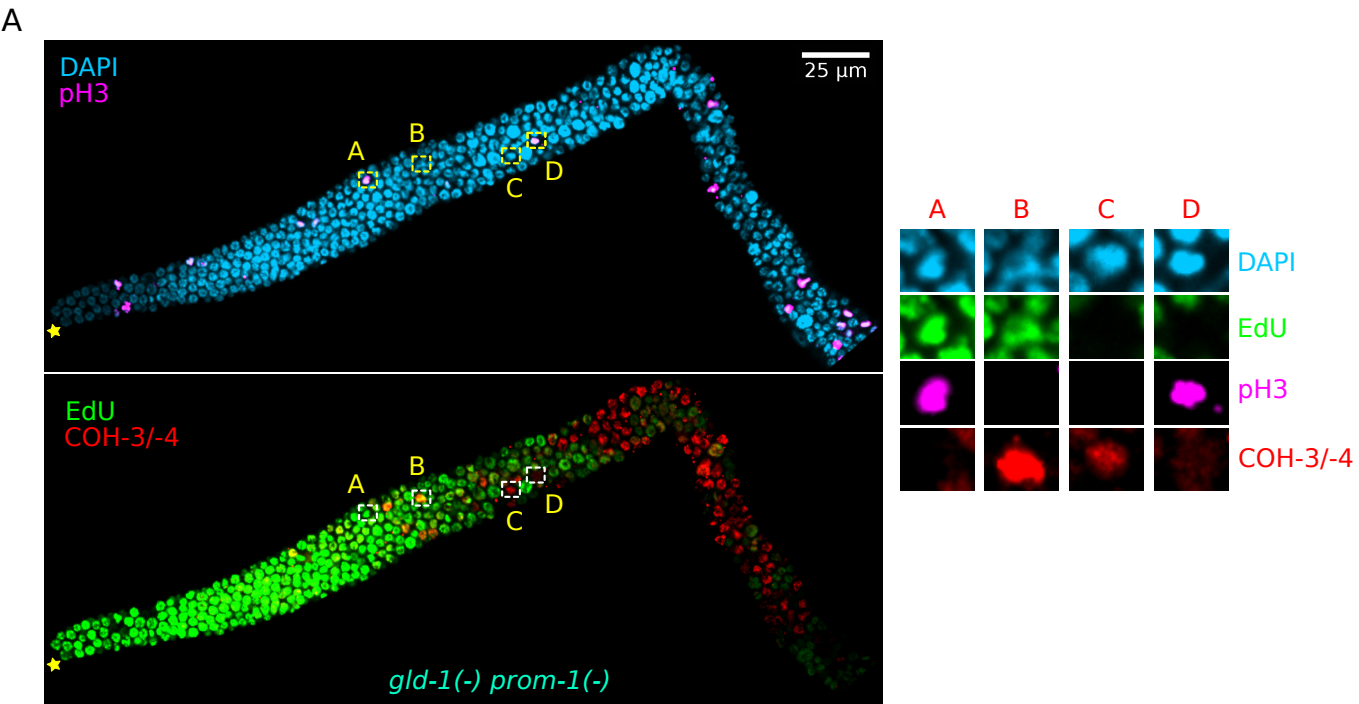
Figure S8



SCF^{PROM-1} male germlines fail to downregulate mitotic cell cycle proteins at meiotic entry.

(A-D) Graphs showing distance, in cell diameter, from distal tip of the germline to last (most proximal) row of cells where the majority of nuclei stain for (A) CYE-1, (B) pCDC-6, (C) WAPL-1 and (D) nucleoplasmic REC-8, for the indicated genotype of young adult male germlines. Data are plotted as horizontal dotplots with each dot representing length in cell diameters to the end of the indicated protein accumulation for one germline. Thick vertical lines represent mean and horizontal lines represent mean \pm std deviation. Statistical significance was determined using either two-tailed Student's T-test (for $n < 30$) or Z-test (for $n \geq 30$). p-value ≤ 0.01 = significant (*), p-value ≤ 0.001 = very significant (**), p-values ≤ 0.0001 = extremely significant (***) and p-values > 0.01 = non-significant (NS.).

Figure S9



B

Type	EdU	pH3	COH-3/-4	Cell Type
A	+	+	—	Mitotically Cycling Cell
B	+	—	+	Meiotic S-Phase Cell
C	—	—	+	Meiotic prophase Cell
D	—	+	—	Return to Mitosis Cell

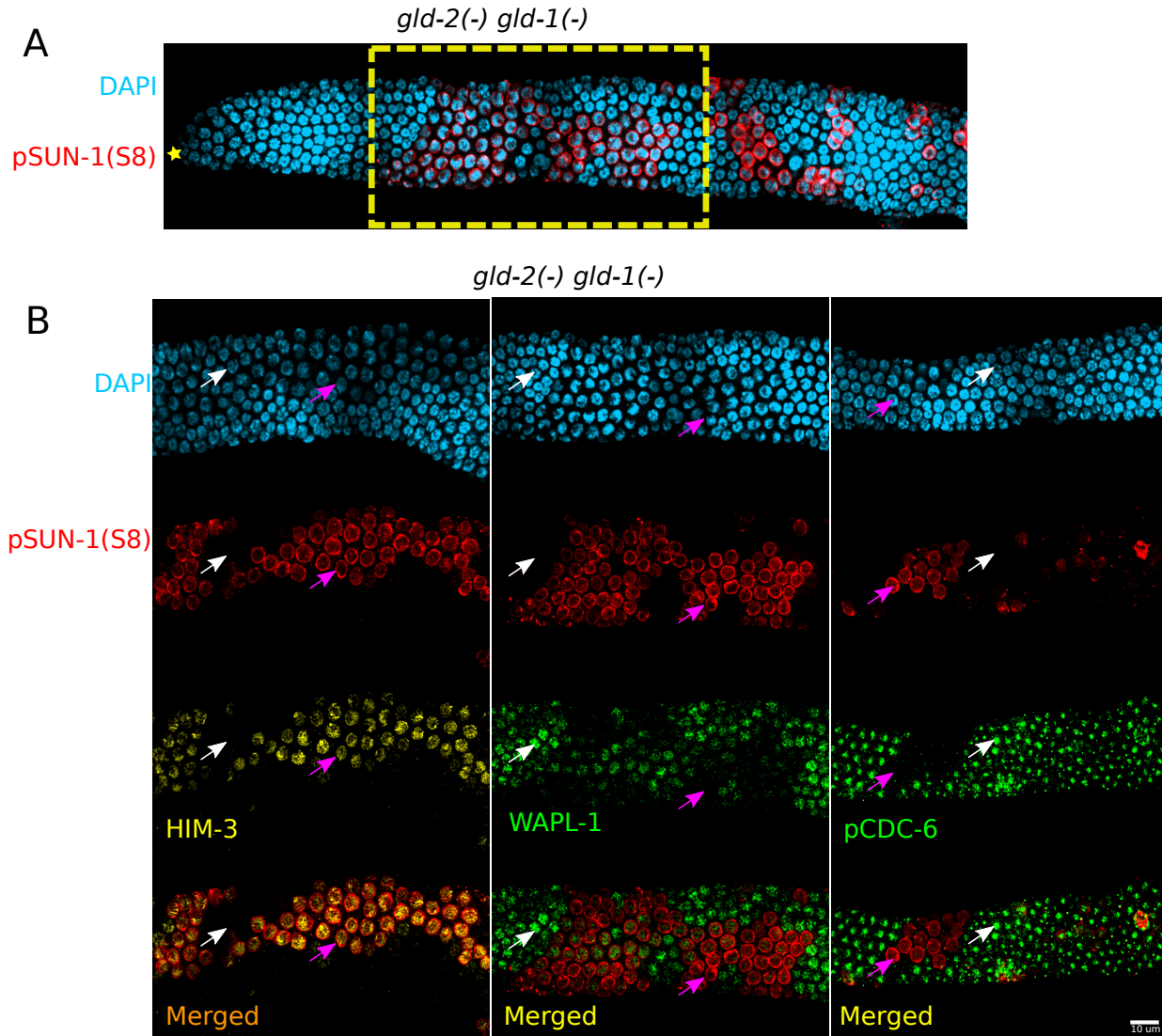
Approach to determine the developmental origin of cells with ectopic mitotic cell cycle activity.

(A) Image of 4-hour EdU labeled (green), co-stained for pH3 (purple), COH-3/-4 (red) and DNA (DAPI, cyan), germline from dissected *gld-1 prom-1* young adult mutant hermaphrodite. Asterisks, distal gonadal end. Inset shows the staining pattern for the four cell types as explained in (B).

(B) Diagram of labeling and staining experiments, results, and four alternative outcomes. Young adult worms are EdU labeled for 4 hours, dissected and stained for EdU incorporation, M-phase (pH3) or meiotic entry (COH-3/4). Prior results (Fox *et al.* 2011) have shown that following a 4 hour EdU labeling, essentially all M-phase cells in the progenitor zone are EdU positive, consistent with the median G2 length of mitotically cycling cells being \sim 2.5 hours, and that a portion of cells that were in meiotic S-phase enter meiotic

prophase (become COH-3/4 or HIM-3 positive) during the time interval. Type - A: M-phase cells (pH3 positive) that are EdU positive, identify cells that are mitotically cycling, having recently undergone a mitotic S-phase (see Figure 5B, C and D). Type B: Meiotic S-phase cells (COH-3/4 or HIM-3 positive) that are EdU positive, identify cells that have recently completed meiotic S-phase. Type C: Meiotic prophase cells (COH-3/4 or HIM-3 positive) that are EdU negative, identify cells that have completed meiotic S-phase prior to EdU labeling and have remained in meiotic prophase during the course of the experiment. Type D: M-phase cells that are EdU negative and are either negative or weakly positive for COH-3/-4 (or HIM-3) identify cells that are preparing to divide, but have not recently undergone an S-phase, suggesting that these cells are returning to mitosis from meiotic prophase. The identification of such cells is confirmed for medial cells in *gld-1* mutant hermaphrodites (Figure S11C), which are known to undergo ectopic proliferation via cells exiting pachytene and returning to mitosis (Francis *et al.* 1995). However, we note that at low frequency M-phase cells that are EdU negative are detected in the progenitor zone, potentially from the small fraction of cells that have a G2 phase that is ~4 hours or longer in length. In the case of *gld-1* mutant hermaphrodites, an 8 hour EdU labeling gave a similar frequency of medial M phase nuclei that were EdU negative, consistent with a return to mitosis phenotype.

Figure S10

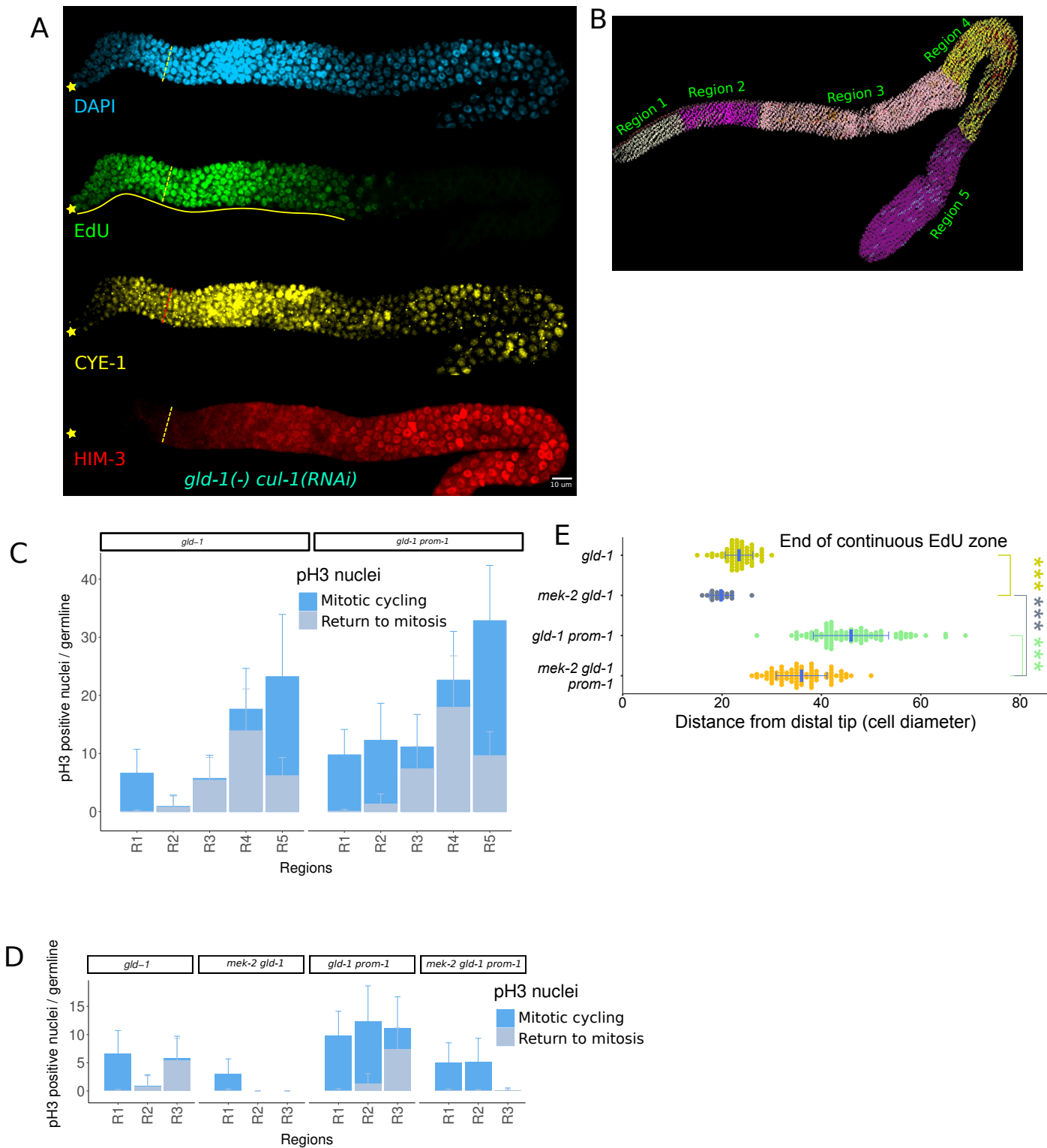


WAPL-1 and pCDC-6 accumulation is downregulated during stochastic meiotic entry that occurs in *gld-2 gld-1* double mutant tumors.

(A) Images of dissected distal germlines from 24 hours old *gld-2 gld-1* mutant hermaphrodites, stained for pSUN-1(S8) (red), and DNA (DAPI, cyan). Yellow box depicts the region of the germlines shown in the (B, below). Asterisks, distal gonadal end.

(B) Regions of *gld-2 gld-1* mutant germlines showing meiotic entry, co-stained with DAPI (cyan). Left panel: co-localization of pSUN-1(S8) (red) and HIM-3 (yellow, bottom left), indicating that pSUN-1(S8) can be used to mark cells that have entered meiosis in *gld-2 gld-1* mutant germlines. Middle panel: co-staining of pSUN-1(S8) (red) and WAPL-1 (green). Right panel: co-staining of pSUN-1(S8) (red) and pCDC-6 (green). Mutually exclusive staining of mitotic and meiotic markers; both WAPL-1 and pCDC-6 nuclear staining disappears upon meiotic entry (cells that are pSUN-1(S8) positive). Asterisks, distal gonadal end. Pink arrows, pSUN-1(S8) positive nuclei. White arrows, pSUN-1(S8) negative nuclei.

Figure S11



Extended EdU zone in *gld-1 prom-1* hermaphrodite germlines is comprised of mitotically cycling cells that have failed to enter meiosis.

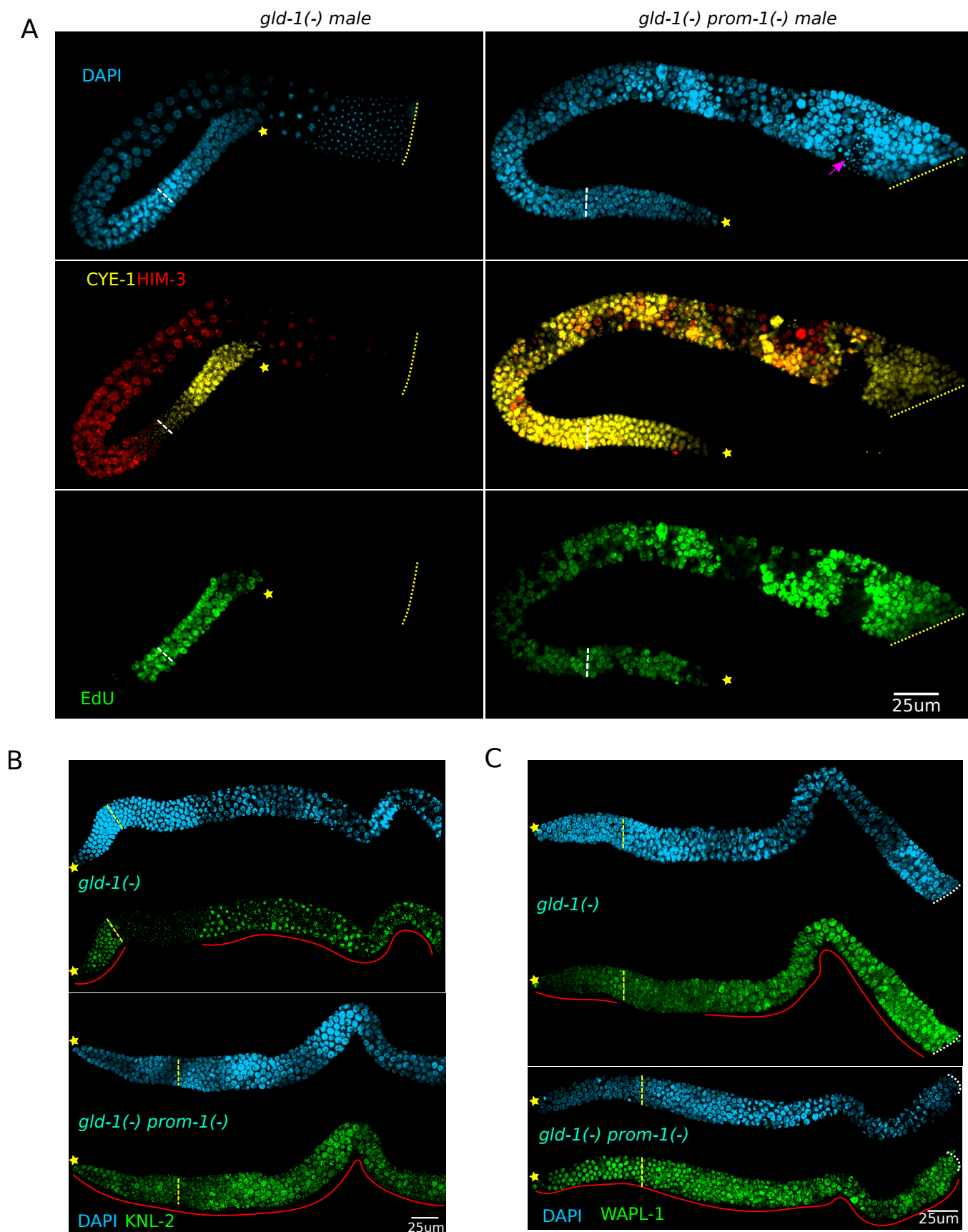
(A) Image of a germline from a dissected *gld-1 cul-1(RNAi)* young adult hermaphrodite EdU labeled for 4 hours (green) and co-stained for CYE-1 (yellow), HIM-3 (red) and DNA (DAPI, cyan). Asterisks, distal gonadal end. Dashed yellow lines, position of overt meiotic entry. Solid yellow line, continuous EdU zone. Note the extended EdU zone as well as accumulation of CYE-1 throughout the germline.

(B) Diagram showing division of the germline into 5 regions for scoring mitotic activity. Region 1 starts from distal end of the gonad to first 20-cell diameter. Region 2 is next 20 cell diameters. Region 3 extends from cell diameter 41 to ~15 cell diameters before loop. Region 4 is essentially 15-cell diameter on either side of loop. Region 5 is the proximal tumor bulb.

(C, D) Bar graph showing number of pH3 positive nuclei that are either EdU positive or negative in (C) Regions 1-5 and (D) Regions 1-3 in hermaphrodite germlines with the indicated genotype. The gonads were divided into regions as above (B). pH3 positive nuclei were counted for each region and classified into either arising from mitotically cycling (EdU positive; blue) cell or return to mitosis (EdU negative; gray) cell based on criteria described in Figure S9. As the number of mitotically cycling cells in Region 2 is similar to Region 1 in *mek-2 gld-1 prom-1* triple mutants, the ectopic proliferation arises from continued mitotic cycling from the progenitor zone, rather than a return to mitosis from meiotic prophase. Data is shown for 22 germlines for *gld-1* and *gld-1 prom-1*, 28 germlines for *mek-2 gld-1* and 90 germlines for *mek-2 gld-1 prom-1*. Error bars, std deviation.

(E) Graph showing continuous EdU zone length, in cell diameters from the distal tip, for young adult hermaphrodite germlines of the indicated genotype. Data are plotted as horizontal dotplots with each dot representing length in cell diameter for one gonad. Thick vertical lines represent mean and horizontal lines represent mean \pm std deviation. Statistical significance was determined using either two-tailed Student's T-test (for $n < 30$) or Z-test (for $n \geq 30$). p-value ≤ 0.01 = significant (*), p-value ≤ 0.001 = very significant (**), p-values ≤ 0.0001 = extremely significant (***) and p-values > 0.01 = non-significant (NS.).

Figure S12

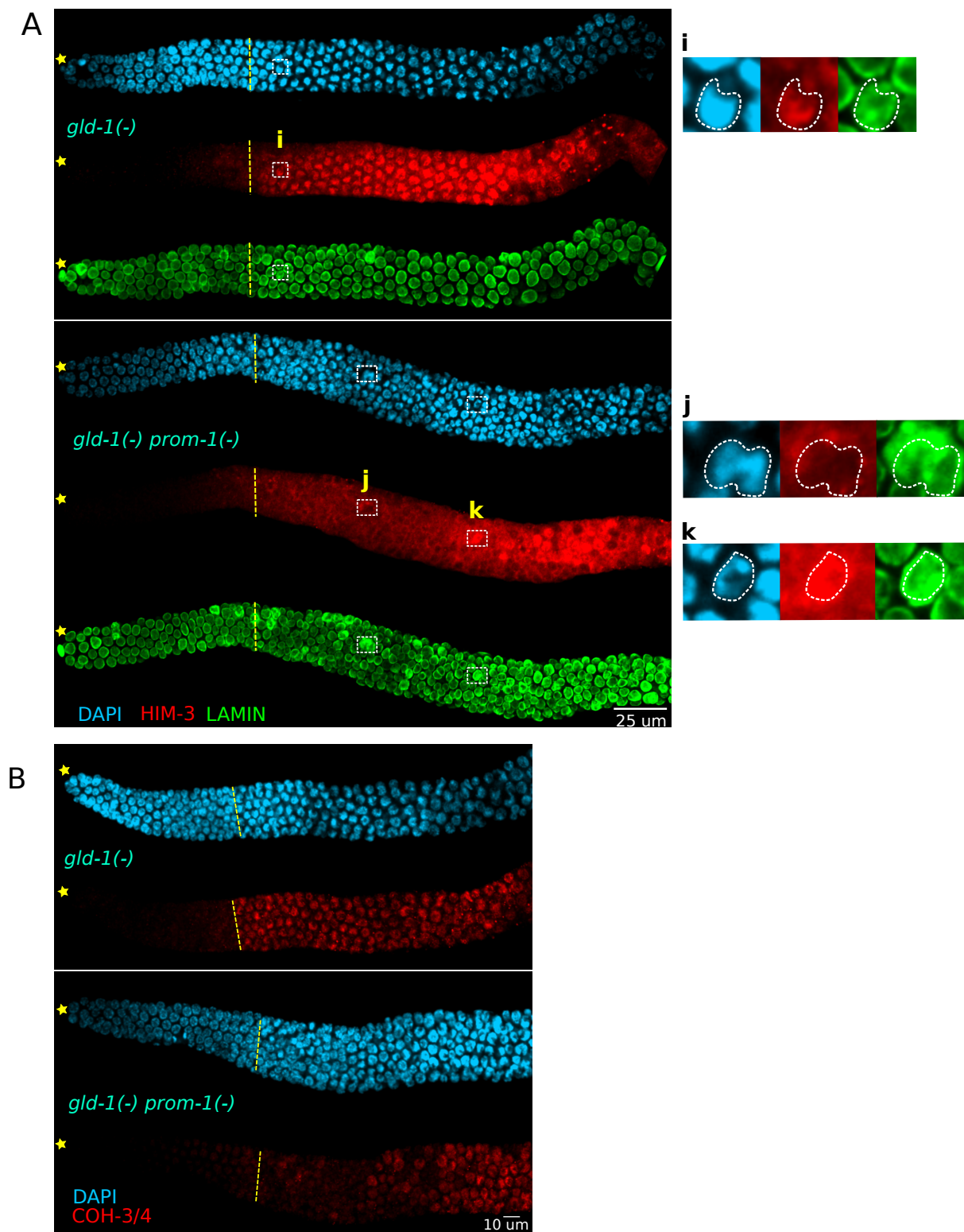


Ectopic mitotic activity in *gld-1 prom-1* mutant males and hermaphrodites.

(A) Images of *gld-1* (left) or *gld-1 prom-1* (right) mutant germlines from dissected young adult males, EdU labeled for 4 hours (green) and co-stained for CYE-1 (yellow), HIM-3 (red) and DNA (DAPI, cyan). Asterisks, distal gonadal end. Dashed white lines, position of overt meiotic entry. Dotted yellow lines, proximal end of the germline. Pink arrow (DAPI stained panel) in *gld-1(-) prom-1(-)* males indicates a pocket of spermatogenesis.

(B, C) Images of (B) KNL-2 (green) and (C) WAPL-1 (green), co-stained with DAPI (cyan), distal gonad arms from dissected young adult hermaphrodites with the indicated genotype. Asterisks, distal gonadal end. Dashed yellow lines, position of overt meiotic entry. Solid red lines, protein accumulation. Dotted white lines, proximal end of the germline.

Figure S13

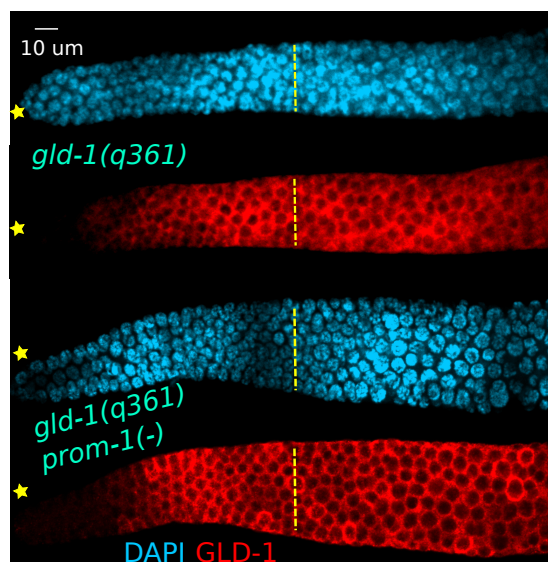


Accumulation of meiotic chromosome axis proteins in *gld-1 prom-1* mutant.

(A) Images of the distal germlines from dissected young adult hermaphrodites of the indicated genotypes stained with antibodies against HIM-3 (red), nuclear lamin (green) and co-stained DAPI (cyan). Insets (right panels) show (i) an early meiotic prophase nucleus from *gld-1* germline where HIM-3 colocalizes with DNA (marked by dashed box in left panel), (j) an early meiotic prophase nucleus from *gld-1 prom-1* germline where HIM-3 accumulates but is not associated with DNA (marked by dashed box) [note that cells in this region of the germline are mitotically cycling], (k) a mid-pachytene nucleus from *gld-1 prom-1* germline with HIM-3 colocalizing with DNA (marked by dashed box). Asterisks, distal gonadal end. Dashed yellow lines, position of overt meiotic entry.

(B) Images of the distal germline from dissected young adult hermaphrodites for the indicated genotype stained with antibodies for COH-3/4-stained (red), co-stained with DAPI (cyan). Asterisks, distal gonadal end. Dashed yellow lines, position of overt meiotic entry. COH-3/-4 accumulates in nuclei in the "early meiotic prophase" region of *gld-1 prom-1* mutants, but the staining intensity is lower and variable [note that cells in this region of the germline are mitotically cycling].

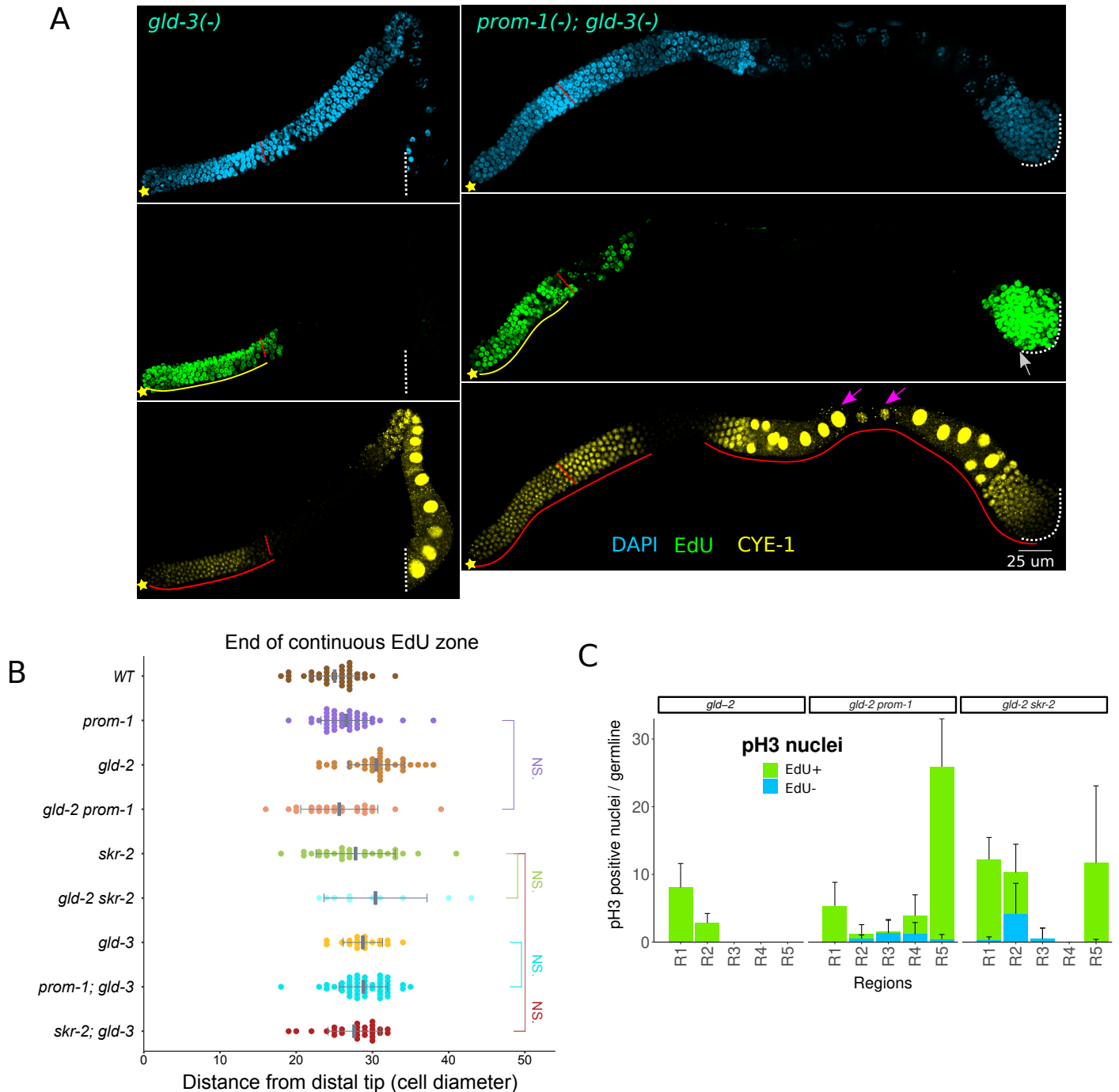
Figure S14



Accumulation of GLD-1 protein in *gld-1 prom-1*.

Images of distal germlines from dissected young adult hermaphrodites with the indicated genotype stained for GLD-1 (red) and co-stained with DAPI (cyan). *gld-1(q361)* makes stable full length GLD-1 that is non-functional. Asterisks, distal gonadal end. Dashed yellow lines, position of overt meiotic entry.

Figure S15



SCF^{PROM-1} interacts with the GLD-2 pathway to promote meiotic entry.

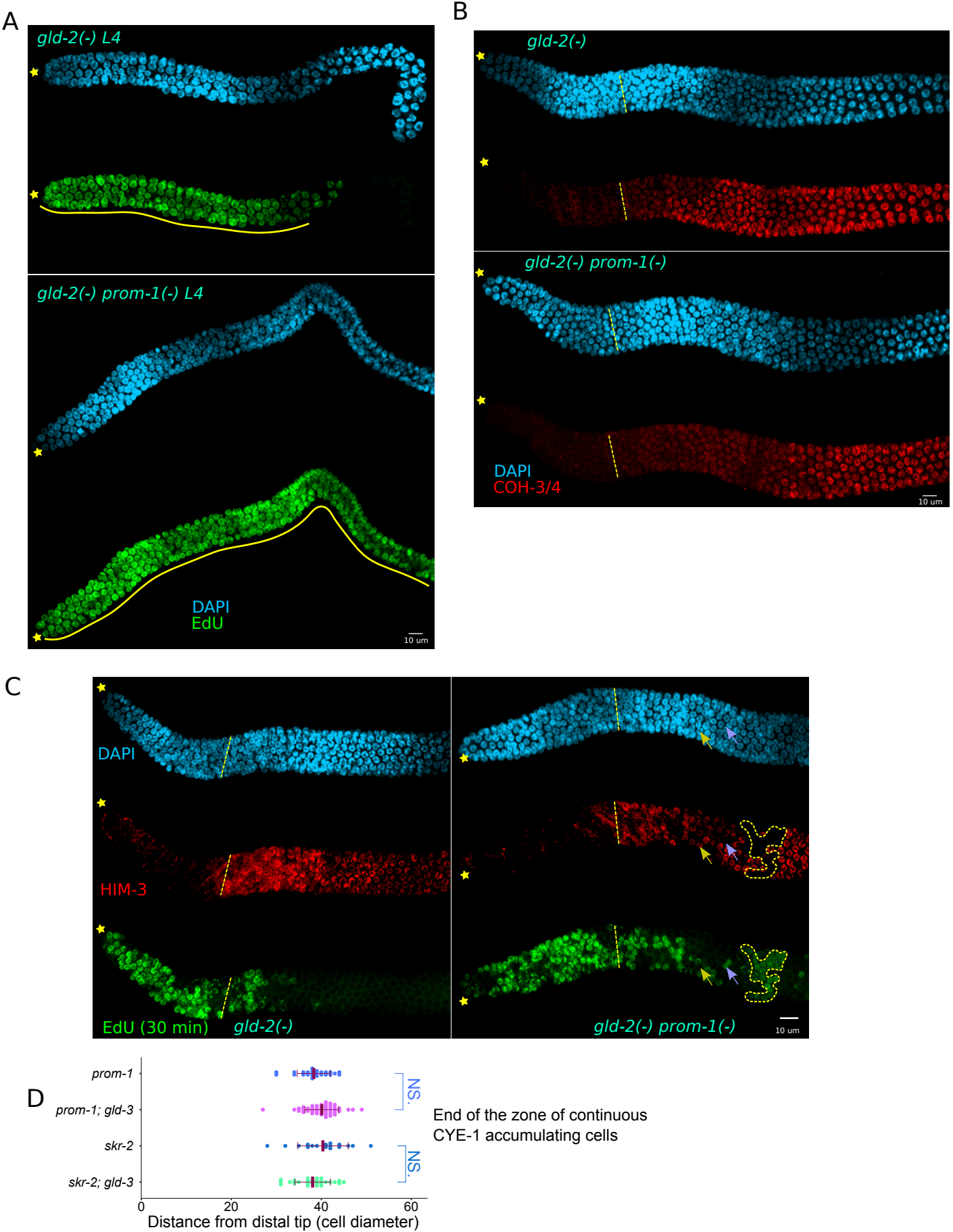
(A) Images of dissected germlines from young adult hermaphrodites of the indicated genotype, labeled with EdU for 4 hours (green), and co-stained for CYE-1 (yellow) and DAPI (cyan). Asterisks, distal gonadal end. Dashed yellow lines, position of overt meiotic entry. Solid yellow lines, continuous EdU zone. Solid red lines, CYE-1 accumulation. White arrow, proximal proliferation. Dotted white lines, proximal end of the germline. Pink arrows, late stage oocyte-like cells.

(B) Graph showing continuous EdU zone length, in cell diameters from the distal tip, for the indicated genotype of young adult hermaphrodite germlines. Data are plotted as horizontal dotplots with each dot representing length in cell diameter for one gonad. Previous studies have shown that *gld-2* and *gld-3* single mutants have longer progenitor zones (Eckmann *et al.* 2002; Fox and Schedl 2015). Thick vertical lines represent mean and horizontal lines represent mean \pm std deviation. Statistical significance was determined using either two-tailed Student's T-test (for $n < 30$) or Z-test (for $n \geq 30$). p -value ≤ 0.01 = significant (*), p -value ≤ 0.001 = very significant (**), p -values ≤ 0.0001 = extremely significant (***) and p -values > 0.01 = non-significant (NS.).

(C) Bar graph showing number of pH3 positive nuclei in regions 1-5 in the hermaphrodite germlines of the indicated genotype. The

gonads were divided into regions as in Figure S11. pH3 positive nuclei were counted for each region and classified into either arising from mitotically cycling (green) or possible return to mitosis (blue) based on logic described in Figure S9. Data is shown for 12 germlines for *gld-2*, 11 germlines for *gld-2 prom-1* and 10 germlines for *gld-2 skr-2*. Error bars, std deviation.

Figure S16



Characteristics of *gld-2* or *gld-3* *SCF^{PROM-1}* double mutant germlines: EdU labeling, accumulation of meiotic chromosome axis proteins and CYE-1.

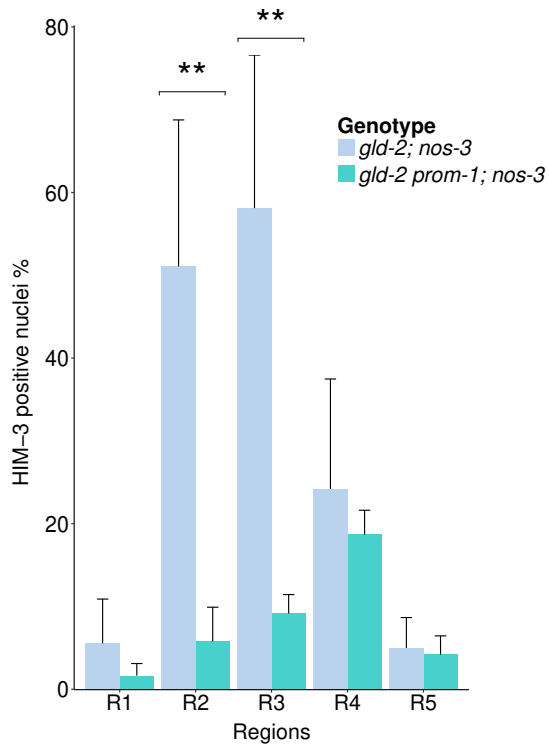
(A) Images of germlines from dissected mid-L4 hermaphrodites of the indicated genotype, EdU labeled for 4 hours (green) and co-stained with DAPI (cyan). Asterisks, distal gonadal end. Solid yellow line, continuous EdU zone.

(B) Images of distal germlines from dissected young adult hermaphrodites of the indicated genotype stained for COH-3/4 (red) and DAPI (cyan). Asterisks, distal gonadal end. Dashed yellow line, position of overt meiotic entry.

(C) Images of distal germlines from dissected young adult hermaphrodites of the indicated genotype, EdU labeled for 30 min (green), stained for HIM-3 (red) and co-stained with DAPI (cyan). Asterisks, distal gonadal end. Dashed yellow line, position of overt meiotic entry. Yellow arrow, HIM-3 positive, EdU negative nucleus. Violet arrow, EdU positive, HIM-3 negative nucleus. Dashed enclosure, a group of nuclei that are EdU positive and HIM-3 negative.

(D) Graph showing distance, in cell diameters from distal tip of the germline to last row where majority of cells are CYE-1 positive, for the indicated genotype of young adult hermaphrodite germlines. Data are plotted as horizontal dotplots with each dot representing length in cell diameter for one gonad. Thick vertical lines represent mean and horizontal lines represent mean \pm std deviation. Statistical significance was determined using either two-tailed Student's T-test (for $n < 30$) or Z-test (for $n \geq 30$). p-value ≤ 0.01 = significant (*), p-value ≤ 0.001 = very significant (**), p-values ≤ 0.0001 = extremely significant (***) and p-values > 0.01 = non-significant (NS.).

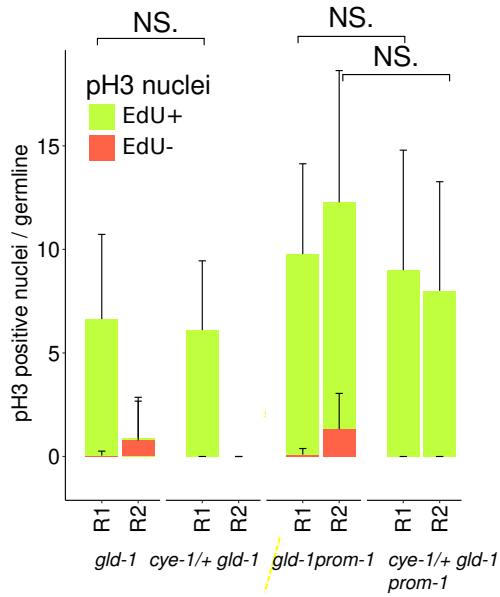
Figure S17



Loss of SCF^{PROM-1} enhances the meiotic entry defect of the *gld-2; nos-2* double mutant.

Bar graph showing mean meiotic index in young adult hermaphrodite germlines for the indicated genotype. The germlines, stained for HIM-3 and DAPI, were divided into 5 regions as shown in Figure S11B. Total nuclei and HIM-3 positive nuclei were counted for each region. Numbers were pooled for each region from 6 gonads of each genotype, and an average “percent HIM-3 positive nuclei” was calculated for each region. Error bars, std deviation. Statistical significance was determined using either two-tailed Student’s T-test (for $n < 30$) or Z-test (for $n \geq 30$). p-value ≤ 0.01 = significant (*), p-value ≤ 0.001 = very significant (**), p-values ≤ 0.0001 = extremely significant (***) and p-values > 0.01 = non-significant (NS.).

Figure S18



Reduction of *cye-1* dose does not affect cell cycle kinetics in *gld-1* and *gld-1 prom-1* mutant germlines.

Bar graph showing mean pH3 positive nuclei in Regions 1 & 2, in young adult hermaphrodites, labeled with EdU for 4 hours, of the indicated genotype. The germlines were divided into regions as in Figure S11B. pH3 positive nuclei were counted for each region separately. Data is shown for 22 germlines each for *gld-1*, *gld-1 prom-1* and 10 germlines each for *cye-1/+ gld-1*, *cye-1/+ gld-1 prom-1*. Error bars, std deviation. Statistical significance was determined using either two-tailed Student's T-test (for $n < 30$) or Z-test (for $n \geq 30$). p-value ≤ 0.01 = significant (*), p-value ≤ 0.001 = very significant (**), p-values ≤ 0.0001 = extremely significant (***) and p-values > 0.01 = non-significant (NS.). There is an expected drop in pH3 positive nuclei in the Region 2 (R2) of *cye-1/+ gld-1 prom-1* compared to *gld-1 prom-1* due to reduction in the size of continuous EdU zone (although the drop is not statistically significant, the p-value is 0.06).

Figure S19

Genotype	PZ	L-Z	Early-pachytene	Mid-pachytene	Late-pachytene	Loop
Wild Type	<div></div>				<div></div>	
SCF ^{PROM-1}	<div></div>	<div></div>			<div></div>	
<i>gld-1</i>	<div></div>		<div></div>	<div></div>	<div></div>	
<i>gld-1 prom-1</i>	<div></div>	<div></div>	<div></div>	<div></div>	<div></div>	<div></div>

Control of mitotic cell cycle proteins by GLD-1 and SCF^{PROM-1}.
Accumulation pattern of mitotic cell cycle proteins (CYE-1, WAPL-1 and KNL-2) in *gld-1*, *SCF^{PROM-1}* and *gld-1 SCF^{PROM-1}* loss of function germlines. PZ, progenitor zone. L-Z, leptotene-zygotene region. The regulation of protein level could be directly controlled (CYE-1) or may be indirectly controlled (WAPL-1, KNL-2).

Literature Cited

- Brenner, J. L. and T. Schedl, 2016 Germline stem cell differentiation entails regional control of cell fate regulator GLD-1 in *Caenorhabditis elegans*. *Genetics* **202**: 1085–1103.
- Eckmann, C. R., B. Kraemer, M. Wickens, J. Kimble, S. Fields, *et al.*, 2002 GLD-3, a bicaudal-C homolog that inhibits FBF to control germline sex determination in *C. elegans*. *Developmental cell* **3**: 697–710.
- Fox, P. M. and T. Schedl, 2015 Analysis of germline stem cell differentiation following loss of GLP-1 notch activity in *Caenorhabditis elegans*. *Genetics* **201**: 167–184.
- Fox, P. M., V. E. Vought, M. Hanazawa, M.-H. Lee, E. M. Maine, *et al.*, 2011 Cyclin E and CDK-2 regulate proliferative cell fate and cell cycle progression in the *C. elegans* germline. *Development (Cambridge, England)* **138**: 2223–2234.
- Francis, R., M. K. Barton, J. Kimble, and T. Schedl, 1995 *gld-1*, a tumor suppressor gene required for oocyte development in *Caenorhabditis elegans*. *Genetics* **139**: 579–606.
- Jantsch, V., L. Tang, P. Pasierbek, A. Penkner, S. Nayak, *et al.*, 2007 *Caenorhabditis elegans* *prom-1* is required for meiotic prophase progression and homologous chromosome pairing. *Molecular biology of the cell* **18**: 4911–20.
- Kipreos, E. T. and M. Pagano, 2000 The F-box protein family. *Gen Biol* **1**: REVIEWS3002.